Proceedings of the 20th International Conference on Soil Mechanics and Geotechnical Engineering– Rahman and Jaksa (Eds)

Stability of axially cyclic loaded displacement piles in sands

Stabilité des pieux battu ou foncés chargés axialement cycliques dans les sables

Siya Rimoy
University of Dar es Salaam, Lecturer in the Department of Transportation and Geotechnical Engineering, United Republic of Tanzania, rimoy@udsm.ac.tz

Matias Silva
Federico Santa Maria Technical University, Assistant Professor in the Department of Civil Engineering, Chile

Richard Jardine
Imperial College London, Professor in the Department of Civil and Environmental Engineering, United Kingdom

ABSTRACT: A wide range of onshore and offshore structures rely on displacement pile foundations. While their critical loading conditions may include significant axial cyclic loading, no internationally agreed guidance exists to guide cyclic design for displacement piles installed in sands or other geomaterials. Field testing provides the best route for developing or calibrating suitable approaches, but such studies are both costly and difficult to conduct. This paper reports an extended investigation that contributes by reporting heavily instrumented laboratory experiments run on 1m long, 36mm diameter close-ended model piles in 1.20m diameter, 1.50m deep, fully pressurised calibration chamber. Tests on Fontainebleau NE34 and GA39 sands explored the potential influences of density, extended load cycles, loading regimes, calibration chamber boundary conditions and installation procedures on the cyclic stability of displacement piles in sands. It has proved possible to link the behaviour observed in the field and model tests to laboratory element model pile tests and the work described contributes towards developing guidance the axial loading design of piles.

RÉSUMÉ: Une large gamme de structures onshore et offshore repose sur des fondations sur pieux. Bien que leurs conditions de chargement critiques puissent inclure une charge cyclique axiale importante, il n'existe aucune directive acceptée au niveau international pour guider la conception cyclique des pieux à déplacement installés dans des sables ou d'autres géomatériaux. Les essais sur le terrain constituent la meilleure voie pour développer ou calibrer des approches appropriées, mais ces études sont à la fois coûteuses et difficiles à mener. Cet article rapporte une enquête approfondie qui contribue en rapportant des expériences de laboratoire fortement instrumentées menées sur des pieux modèles fermés de 1 m de long et 36 mm de diamètre dans une chambre d'étalonnage entièrement pressurisée de 1,20 m de diamètre, 1,50 m de profondeur. Les essais sur les sables de Fontainebleau NE34 et GA39 ont exploré les influences potentielles de la densité, des cycles de charge prolongés, des régimes de chargement, des conditions aux limites de la chambre d'étalonnage et des procédures d'installation sur la stabilité cyclique des pieux à déplacement dans les sables. Il s'est avéré possible de lier le comportement observé sur le terrain et les essais sur modèle aux essais de pieux sur des modèles d'éléments de laboratoire et les travaux décrits contribuent à développer des orientations pour la conception de chargement axial des pieux.

KEYWORDS: Displacement piles, sand, cyclic loading

1 INTRODUCTION

An ability to sustain axial cyclic loading can be critical to pile foundations particularly in offshore energy applications. However, internationally agreed design guidance for such conditions is yet to be achieved. Puech and Garnier (2017) report the French National SOLCYP programme that developed axial cyclic design methodologies from monotonic-and-cyclic field tests on displacement and bored piles in stiff clays and marine sands. The reference data for piles driven in sands was multiple one–way (OW) tension and two–way (TW) tension and compression cyclic experiments conducted by Jardine and Standing (2012) on seven, 457mm outside diameter, mostly 19m long, open steel piles which were driven in medium-to-fine dense Dunkirk sand, in northern France. The outcomes of the Dunkirk axial cyclic tests are summarised in Figure 1 by an interactive stability diagram which shows how outcomes depend on the combination of mean pile head load (Q_{mean}) and cyclic amplitude (Q_{cyclic}) relative to the tension shaft capacity (Q_T), and number (N) of cycles and categorises the responses to regular cycling as being:

a) *Stable (S)*, where pile head axial displacements accumulate very slowly over thousands of cycles and there is no significant loss of shaft capacity, or
b) *Unstable (US),* where displacements accumulate relatively rapidly and shaft capacity falls to give failure within 100 cycles, or
c) *Meta-Stable (MS),* where displacements accumulate at moderate rates without stabilising. Capacity losses accrue that lead to failure after 100s or 1000s of cycles.

Rimoy et al. (2013) analysed the piles' axial cyclic load-displacement and stiffness responses, finding that cyclic stiffness loss (and transient displacement growth) was only significant as failure was approached under unstable or metastable conditions where pile movements grew relatively rapidly. Stable cycling led to minimal displacement accumulation. The Dunkirk field tests provided a unique dataset, but they do not show how different sand conditions might affect cyclic performance. It was also impossible to measure soil contact stresses on the Dunkirk piles' surfaces, or in the sand mass. Extending the tests to cover more than 1000 cycles was also unfeasible.

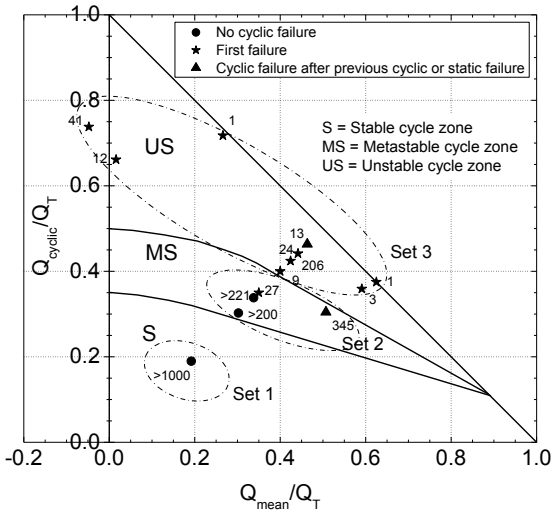

Figure 1. Axial cyclic interaction diagram for the full–scale pile tests in Dunkirk silica marine sands (Jardine & Standing 2012).

Rimoy et al. (2015) reported experiments with 1m long, 36mm diameter model piles in the 1.20m diameter, 1.50m deep, fully pressurised Grenoble-INP calibration chamber, aiming to study more fundamentally the phenomena observed in the field. The experiments were run under strictly controlled environmental conditions, with multiple miniature sensors gauging the local stresses both on the pile shaft and in the dry sand employed: see Jardine et al. (2009) and Zhu et al. (2009). Crucial differences between field and laboratory behaviour soon became evident. Rimoy et al. (2015) noted that the model piles did not display the same marked growth of shaft capacities in the weeks to months that followed installation. Carroll et al. (2020) ascribed this to (i) physio-chemical conditions being different in the laboratory and (ii) potential scale and geometrical effects that result from the finite thicknesses of zones of crushed sand grains formed around the walls of open tubular steel piles. Nevertheless, the model tests offered new insights into the effective stress conditions developed during installation, static load testing and under repetitive loading (with up to 1000 cycles) in dense dry silica Fontainebleau NE34 sand. This paper reports further model experiments conducted by Rimoy (2013) and Silva (2014) with similar systems that explored the potential influences on cyclic behaviour of:

1) Different sands and density states
2) Calibration chamber boundary conditions
3) Larger numbers of cycles and a wider range of loading regimes
4) Modes of installation modes by either driving or jacking

2 TESTING SET-UP AND PROGRAMME

Each model pile installation required up to 2.7 tonnes of fresh, air-pluviated sand. Fontainebleau NE34 or GA39 sands were employed, whose index properties are summarised on Table 1. Liu (2018) reports the similarity in mechanical behaviours between Dunkirk sand and NE34 sand to which GA39 sand is broadly similar apart from its grain size. Rimoy et al. (2015) describe the systems which could measure local stresses and loads while maintaining good long-term boundary stress and temperature controls. The sand masses could be tested dry, or after near-saturation with water following CO_2 replacement, employing initial density indices $I_D \approx 40\%$ and 70% for the GA39 and NE34 sands respectively. Vertical pressures of 150 ± 5 kPa were maintained before pile installation, over extended ageing durations and during load testing. A total of 43 cyclic and a similar number of static tests are reported herein from five new installations made with 36mm outer diameter closed-ended driven 'DT' piles equipped with axial load cells and seven with the 36mm outer diameter cone-tipped, stainless steel Mini-Imperial College Pile (Mini-ICP) shown in Figure 2, which records local shaft shear and radial stresses accurately through three sets of Surface Stress Transducers (SSTs) as well as axial loads and temperatures.

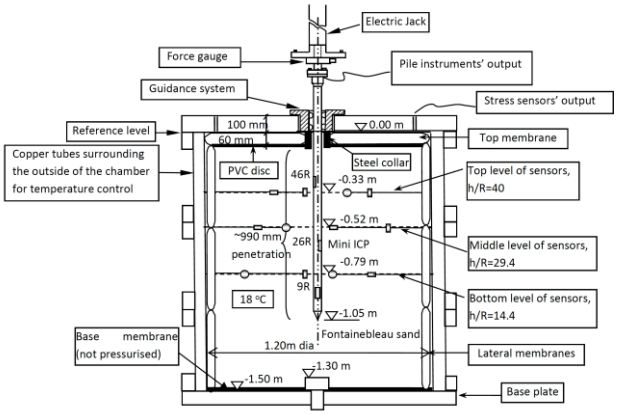

Figure 2. Calibration Chamber and Mini–ICP arrangements of tests ICP07 and 08; vertical section after Rimoy (2013). Pile sensors h=9R above tip are 'Leading', at 26R are 'Following', and at 46R are 'Trailing'.

Figure 3 presents equivalent q_c profile from the continuous monitoring of the Mini-ICP tip load cell during installation. Tests on dry NE34 sand showed q_c profiles of approximately 20 MPa, while the finer GA39 sand showed profiles 10 and 15 MPa for tests ICP05 and ICP10 respectively. The chamber-to-pile diameter ($D_{chamber}/D_{pile}$) ratios was 33.3. Although much lower ratios are frequently adopted, Salgado et al. (1998) argue that field conditions can only be matched in rigid chambers if $D_{chamber}/D_{pile} > 100$. Check tests were therefore undertaken with a range of 'passive' and 'active' conditions (after Huang & Hsu 2005) comprising:

BC1 – Passive stress-controlled radial boundaries, with three depth-segmented water-filled membranes held under constant applied pressure

BC3 – Passive radial rigid-wall, as imposed by the steel chamber boundary

BC5 – Active radial boundaries that replicated 'field conditions' through three depth-segmented water-filled membranes which are isolated to measure the three boundary pressures during installation. The elevated pressures achieved at end of installation were held fixed throughout ageing to compensate for the effects of elastic strain energy stored beyond the limit of the calibration chamber wall in the field.

The model piles were tested at a wide range of ages after their installation. Rimoy et al. (2015) show that the jacked model piles developed age-insensitive capacities in NE34 sand that were generally close to those predicted with the CPT based ICP-05 design methods for driven piles in sands. Loads (or displacements) were cycled by imposing smooth sine waveforms at the pile head at rates between 0.5 and 8.5 cycles per minute. Most of the cyclic tests were conducted under load control following Q_{mean}/Q_T and Q_{cyclic}/Q_T parameters. The cyclic tests' codes signify: first their test series numeral, then an extension denoting the mode (One-Way or Two-Way), followed by the number of tests performed on the pile up to, and including, that stage. Reference shaft capacities (Q_T) were measured through tension testing before most cyclic tests. Tension tests were adopted because they require smaller displacements (usually far less than D/10) than compression tests to reach peak resistance and are simpler to interpret. It is recognised that prior testing on any given pile affected the responses observed in any subsequent test and the reference static tension tests served to track the

impact of prior experiments on axial shaft capacity. Tension loads are reported as having a negative sign.

Table 1. Index properties of NE34 Fontainebleau and GA39 Nemours sand.

Sand	Grain shape	SiO_2 (%)	G_s	d_{10} (mm)	d_{50} (mm)	d_{60} (mm)	C_u	e_{max}	e_{min}
NE34	Sub-angular, sub-rounded	99.70	2.65	0.150	0.210	0.230	1.53	0.90	0.51
GA39	Sub-angular, sub-rounded	98.60	2.65	0.100	0.127	0.132	1.32	1.01	0.56

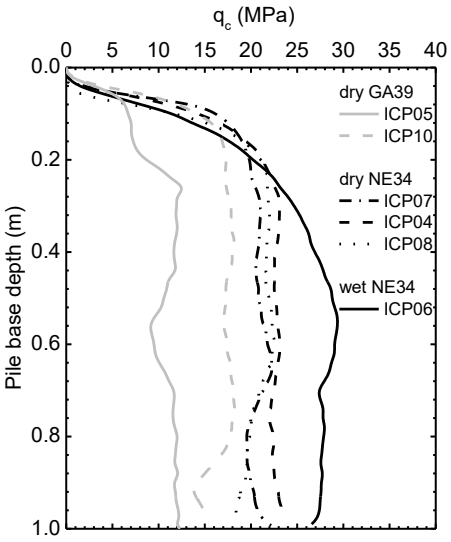

Figure 3. Pile end-bearing resistances for Mini-ICP pile jacked tests in this study.

3 RESULTS AND DISCUSSION

3.1 Stability Interaction Diagrams

Cyclic stability interaction diagrams can summarise how the number of cycles *N* that can be sustained before any failure occurs relate to the cyclic loading conditions.

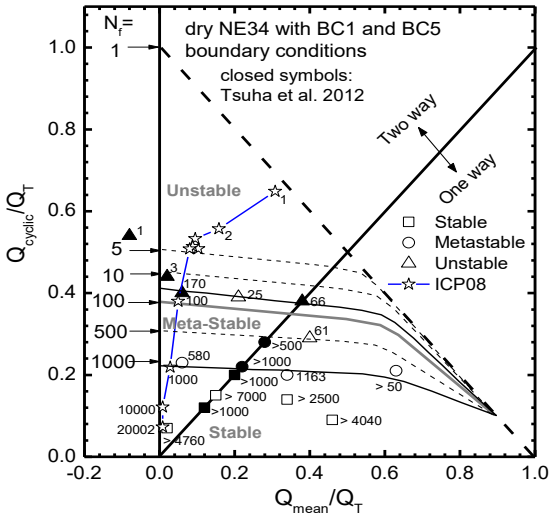

Figure 4. Interaction diagram for the Mini-ICP in dry NE34 sand

The outcomes can be classified according to the accumulated cyclic displacements *a* normalised by the pile diameter *D*, and the derivatives d(a/D)/dN. In this study, tests that sustained at least 1000 cycles, before displacements exceeded 0.01D or rates exceeded to 3D x 10^{-6} mm/cycle and showed no loss in operational static shaft capacity were deemed *Stable* (S), while *Unstable* (US) tests accumulated total displacements greater than 0.1D at rates greater than 3D x 10^{-4} mm/cycle over significant durations, showed significant shaft capacity degradation and generally failed within 100 cycles. *Metastable* (MS) tests showed intermediate displacements, displacement rates and modest shaft capacity degradation that led to failure in hundreds of cycles. While small numbers of such cycles may not affect capacity or serviceability, large numbers cannot be sustained safely. Figure 4 present the Authors' tests, referring their outcomes to the Stable, Metastable Unstable regions identified by Tsuha et al. (2012) for piles jacked cyclically into dry NE34 sand, which manifested a similar pattern to the Dunkirk field tests summarised in Figure 1.

Experiment ICP06 was designed to test whether water influenced the outcomes by installing a Mini-ICP, under B C3 conditions, in near-saturated NE34 sand. Noting that di rect comparison between the earlier dry sand model experi ments and the Dunkirk field tests, which developed most of their capacity below the water table, might be questione d, the displacement-controlled, Two-Way, test ICP06TW1 (+/- 0.5mm) was conducted, followed by the One-Way test ICP06OW1 (Q_{cyclic}/Q_T = Q_{mean}/Q_T = 0.11) which remained *Stable* after 1000 cycles. The tests' normalised outcomes presented in Figure 5 are fully compatible with Tsuha et a l.'s (2012) dry sand tests.

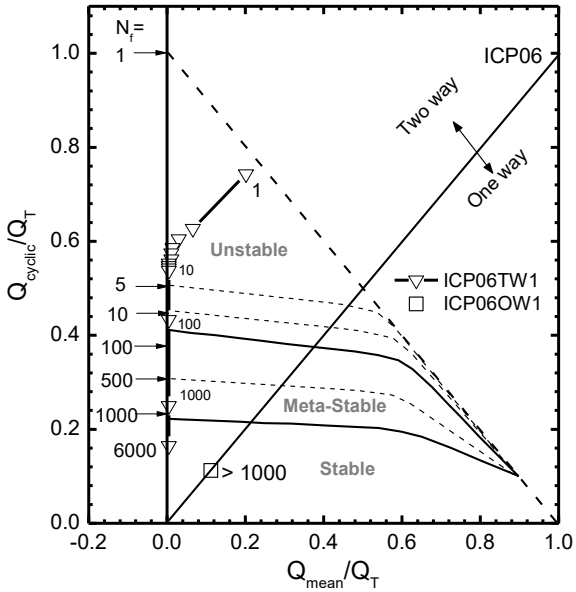

Figure 5. Interaction diagram for ICP06 in wet NE34 sand.

The influence of installation procedure was investigated by driving closed ended 36 mm diameter piles DTIII to DTVII in dry, $I_D \approx 0.70$, NE34 sand under BC1 and BC5 conditions. Twenty-one (OW and TW) cyclic loading tests were performed, yielding the results in Figure 6, with normalised *Unstable*, *Metastable* and *Stable* boundaries that plot far below those manifested by both the jacked model piles (Figure 4 & 5) and the Dunkirk field tests presented in Figure 1. The tests also gave lower absolute capacities than expected. Overall, the driven model test conditions fail to represent those applying in the field.

3.2 Local stress variations induced at pile interface and in sand mass by axial cyclic loading

The Mini-ICP piles' instrumentation allowed the jacked piles' cyclic local shear stress τ_{rz} versus normal radial effective stress σ'_r stress paths to be followed at the sand-pile interface, which

was not possible with the field or laboratory driven piles. It was also possible to follow the stress paths invoked within the surrounding sand mass. Tsuha et al. (2012) reported on the paths followed at three levels on the shaft in dry ($I_D \approx 0.70$) NE34 sand under BC1 and BC3 conditions, showing that stable tests' stress paths remained within an interface failure envelope, for which $\delta \approx 27°$ in accordance with Yang et al's (2011) ring-shear interface tests.

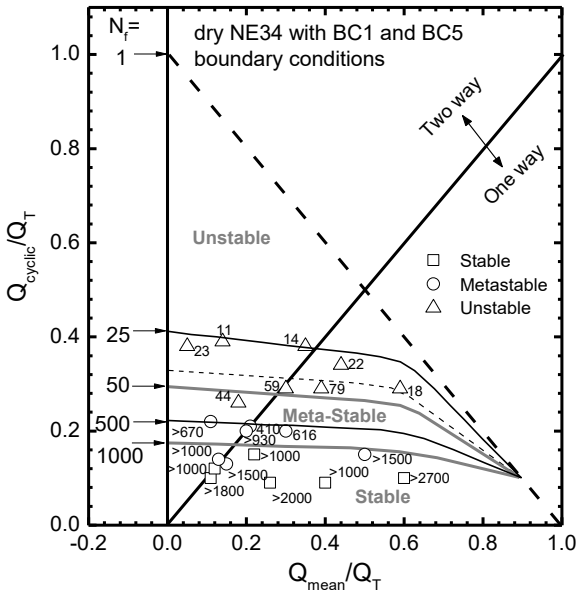

Figure 6. Interaction diagram for driven piles in dry NE34 sand.

Cyclic loading tests undertaken in the ICP05 to 11 experiments revealed similar styles of effective stress responses applied with: (i) a range of calibration chamber boundary conditions, (ii) wet NE34 sand, (iii) finer, looser, dry GA39 sand, (iv) in many tests, after far larger numbers of cycles. Figure 7 and 8 illustrate the impact of the unstable, extreme two-way applied conditions in ICP08 TW1 experiment, considering the first 10 and the final 10 cycles of this 20,002 cycles experiment. Significant differences were observed in (dry) Mini-ICP tests with the finer, loose, GA39 sand, which developed far lower axial resistances and radial shaft shear stresses than were seen with NE34 sand under the same (150 kPa) vertical calibration chamber pressure. The stress changes provoked within the surrounding sand mass by severe two-way cycling are illustrated in Figure 9 by σ'_r measurements made at three normalised radial distances (r/R) from the pile axis at a normalised level h/R = 39.2 vertically above the tip in test TW1 on ICP08. While the pile shaft experiences large (≈ 130 kPa) final losses in σ'_{rs}, significant (≈50 kPa) reductions applied 2 to 8 radii from the axis.

Measurements were also made in BC5 tests of the pressures developed in the chamber's three, vertically stacked, outer radial chamber membranes. The membranes were isolated during the TW1 test on ICP08 and Figure 10 shows that ≈10 kPa in σ'_{rs} developed out at r/R ≈30, confirming that either larger chambers or active boundary conditions (such as the BC5 system) are required to capture the field response in a fully representative manner. In the same line, boundary pressure measurements made with BC5 conditions during installation showed increases during jacked installation (when the membranes were isolated) that contrasted with radial pressures falling sharply at the chamber wall during equivalent driven installations.

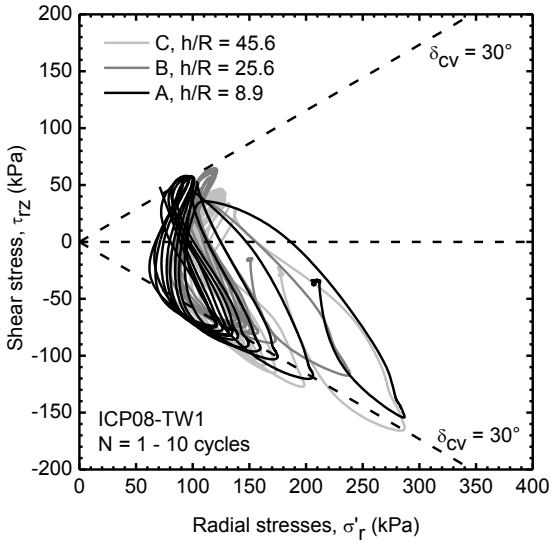

Figure 7. Interface effective stress paths from unstable two-way cyclic loading test ICP08-TW1 (+/- 0.5mm) in dry NE34 sand under BC5 boundary conditions first 10 cycle.

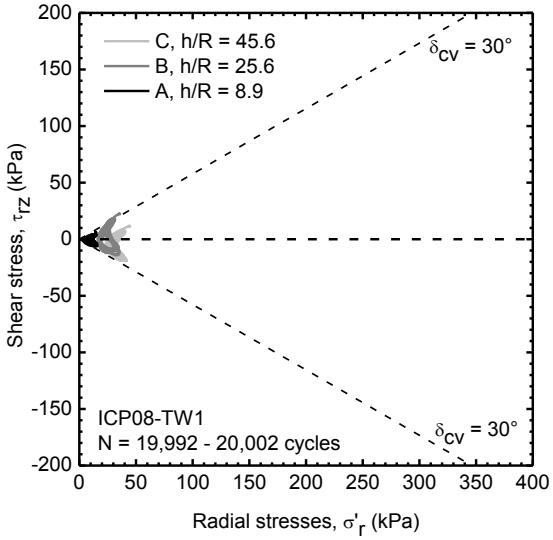

Figure 8. Interface effective stress paths from unstable two-way cyclic loading test ICP08-TW1 (+/- 0.5mm) in dry NE34 sand under BC5 boundary conditions final 10 cycles.

3.3 Axial cyclic stiffness and displacements

Cyclic stiffnesses were tracked by defining a measure $k = (Q_{max} - Q_{min})/d_{cyclic}$ where Q_{max} is the maximum axial cyclic load, Q_{min} is the minimum axial cyclic load and d_{cyclic} the maximum cyclic displacement.

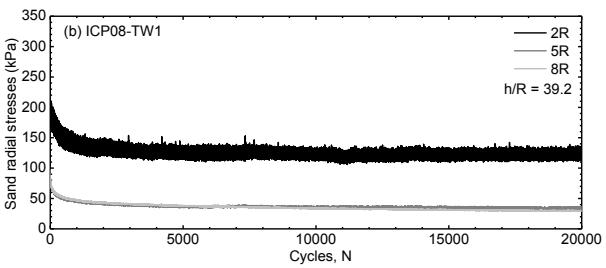

Figure 9. Sand mass radial stresses against the number of cycles applied in unstable two-way cyclic loading test ICP08-TW1 in dry NE34 sand

under +/- 0.5mm displacement control under with BC5 boundary conditions.

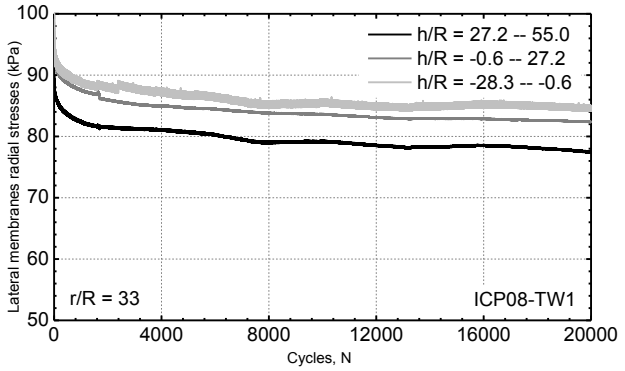

Figure 10. Radial stresses at the calibration chamber boundary against the number of cycles applied in unstable two-way cyclic loading test ICP08-TW1 in dry NE34 sand under +/- 0.5mm displacement control under with BC5 boundary conditions.

Figure 11 shows how loading stiffnesses (and therefore cyclic displacements) remained practically constant up to 10,000 cycles in the stable tests by plotting $k_l/k_{l,N=1}$ against N. The equivalent data from the metastable tests are also shown. Most of the latter also manifested nearly constant stiffness. However, in some cases, such as ICP04-TW1, stiffness degraded by up to 85% as failure approached. The corresponding unstable cyclic loading tests stiffness trends are illustrated in Figure 12. Test ICP05-OW2, ICP11-OW3 and ICP11-TW1 survived to just 74, 61 and 25 cycles respectively and showed cyclic stiffness degrading after just 10 to 30 cycles. Figures 13 and 14 show how the driven piles' normalised stiffnesses varied with number of cycles, giving broadly similar trends to the jacked piles. Overall, no clear difference could be seen between the stiffness degradation trends developed under BC3 or BC5 conditions in wet-or-dry, loose-or-dense sand masses, by jacked or driven piles.

Table 1. Axial cyclic loading test series using Mini-ICP.

Cyclic test series and code	Q_{cyclic}/Q_T	Q_{mean}/Q_T
Stable		
ICP04-OW1	0.15	0.15
ICP06-OW1	0.11	0.11
ICP07-OW1	0.09	0.46
ICP07-TW1	0.07	0.02
ICP11-OW1	0.14	0.34
Metastable		
ICP04-TW1	0.23	0.06
ICP04-OW2	0.21	0.63
ICP05-OW1	0.22	0.38
ICP05-TW1	0.26	0.11
ICP05-TW2	0.24	0.17
ICP10-OW4	0.27	0.28
ICP10-TW2	0.21	0.00
ICP11-OW2	0.20	0.34
Unstable		
ICP05-OW2	0.33	0.40
ICP11-OW3	0.29	0.40
ICP11-TW1	0.39	0.21

3.4 Permanent accumulated cyclic displacements

The permanent cyclic pile-head displacements accumulated during load-controlled cycling are shown in Figures 15 to 17. Naturally, the displacement-controlled tests did not develop permanent displacements.

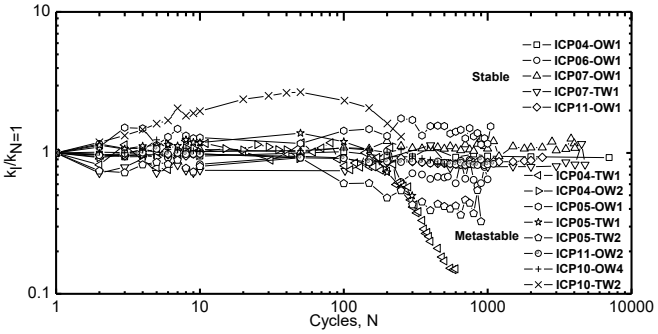

Figure 11. Normalised axial cyclic pile stiffness versus number of cycles applied in stable and metastable cyclic loading tests with ICP pile.

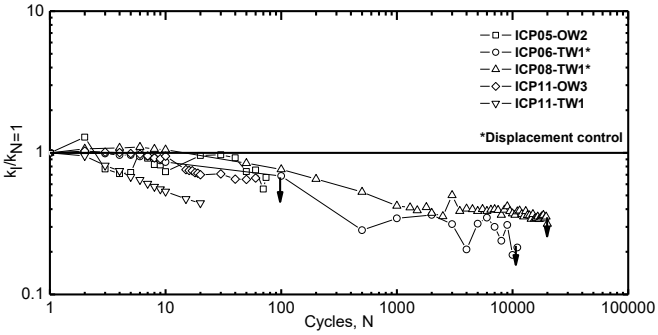

Figure 12. Normalised axial cyclic pile stiffness versus number of cycles applied in unstable cyclic loading tests with ICP pile.

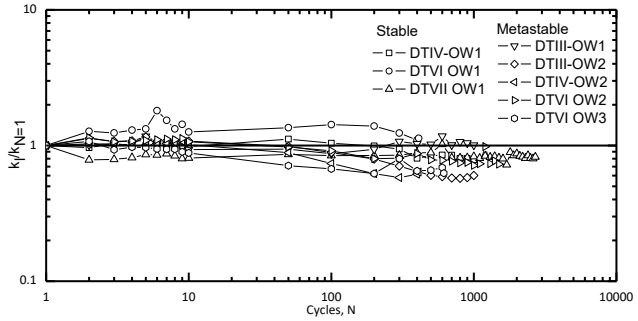

Figure 13. Normalised axial cyclic pile stiffness versus number of cycles applied in stable and metastable cyclic loading tests: driven piles under BC5 conditions.

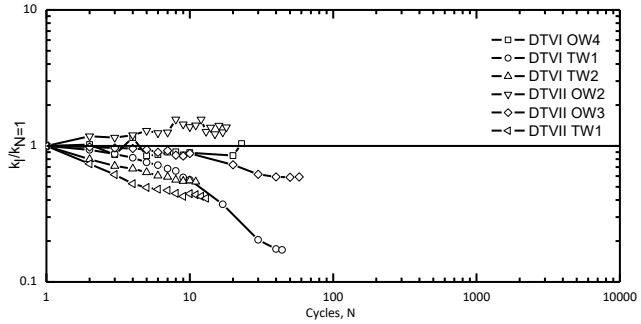

Figure 14. Normalised axial cyclic pile stiffness versus number of cycles applied for in unstable cyclic loading tests: driven piles under BC5 conditions.

The segmented reference lines correspond to the stability criteria discussed earlier, which are broadly consistent with the Dunkirk field tests analysed by Rimoy et al. (2013) although some differences exist in the rates at which the cyclic displacements (divided by diameter D) grew as cyclic failure approached under metastable or unstable conditions. Stable cyclic tests showed almost negligible displacement accumulation rates, independent of the installation method, sand type and density indices.

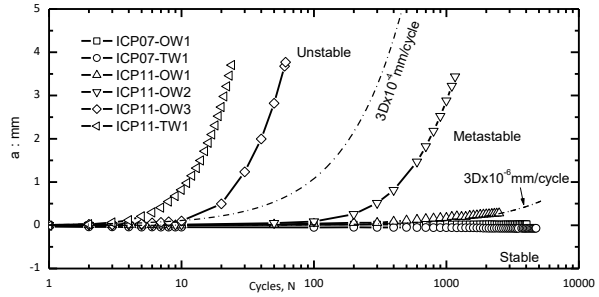

Figure 15. Permanent accumulated cyclic displacement during cyclic loading tests in dry NE34 sand: ICP pile under BC5 conditions.

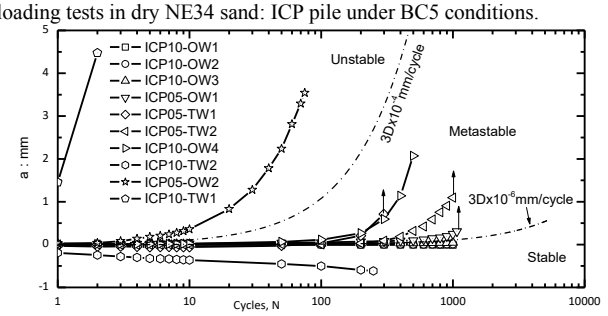

Figure 16. Permanent accumulated cyclic displacement during cyclic loading tests in dry GA39 sand; ICP pile under BC5 conditions.

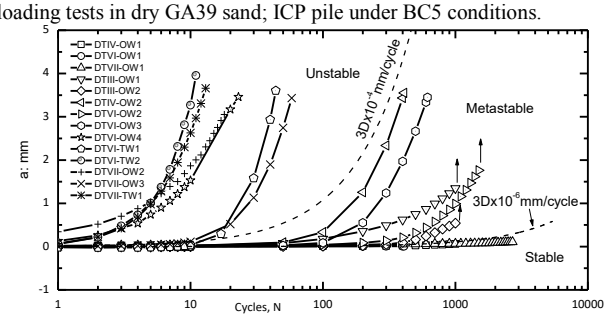

Figure 17. Permanent accumulated cyclic displacement during cyclic loading tests in dry GA39 sand; ICP under BC5 conditions.

4 CONCLUSIONS

This paper addressed uncertainties regarding modelling the axial cyclic behaviour of piles driven in sands, referring to field tests before reporting and interpreting an extended programme of 43, mostly heavily instrumented, calibration chamber cyclic model pile tests supported by multiple static tests. The programme was designed to explore the potential influences of (i) initial conditions in the sand, (ii) large numbers of cycles and a wide range of loading regimes, (iii) calibration chamber boundary conditions and (iv) pile installation by both driving and jacking. The experiments contribute towards developing design guidance for cyclic axial loading cases and lead to six main conclusions:

1. Wet and dry sands placed at the same I_D follow broadly the same trends under regular cyclic loading when the outcomes are considered in terms of the normalised cyclic loading parameters Q_{cyclic}/Q_T, Q_{mean}/Q_T and N.
2. Little or no change in cyclic stiffness occurs when loading remains within a well-defined stable region, even over 10,000 or more cycles. In contrast, unstable tests lose stiffness rapidly and fail dramatically after less than 100 cycles. Metastable tests show intermediate responses that depend on the imposed normalised loading levels.
3. Cyclic damage occurs due to reductions in the radial effective stresses acting on the pile shaft and failure is controlled by interface failure angles.
4. The chamber-to-pile diameter ratio of 33 employed in the present tests leads to significant radial stress variations at the chamber wall, whose impact can be reduced by adopting 'active' BC5 chamber boundary conditions.
5. The jacked Mini-ICP calibration chamber tests in NE34 sand led to broadly similar normalised cyclic stability, stiffness and permanent displacement trends to full-scale field tests (conducted at various ages after driving) in Dunkirk sand, which has similar grain sizes, mechanical properties and in-situ I_D levels to the NE34 sand employed for the model tests.
6. However, the model experiments were unable to capture reliably some of the key features observed in the field, including shaft capacity growth over time, the impact of driven rather than jacked installation and potentially the impact of low relative density sand layers. These outcomes may be unintended consequences of the model pile testing arrangements. Field tests remain the best means of establishing reliable design guidelines.

5 ACKNOWLEDGEMENTS

The authors gratefully acknowledge the sponsorship and provided by the Commonwealth Scholarship, BECAS Chile, Engineering and Physical Sciences Research Council (EPSRC), Centre National de la Recherche Scientifique (CNRS), the Health and Safety Executive (HSE), Shell (UK) and Total France. They also thank their many current and former colleagues at Imperial College and INGP Grenoble as well as Cambridge In-situ for their contributions. In particular, the wish to acknowledge the contribution, support and offshore geotechnics legacy of the late Professor Pierre Foray of Laboratoire-3SR, Grenoble.

6 REFERENCES

Carroll, R., Carotenuto, P., Dano, C., Salama, I., Silva, M., Rimoy, S., Gavin, K., and Jardine, R. (2020). Field experiments at three sites to investigate the effects of age on steel piles driven in sand. *Géotechnique,* **70**(6), pp 469 – 489.

Huang, A., & Hsu, H. (2005). Cone penetration tests under simulated field conditions. *Géotechnique*, **55**(5), pp 345-354.

Jardine, R. J., Zhu, B. T, Foray, P. and Dalton, C. P. (2009). Experimental arrangements for the investigation of soil stresses developed around a displacement pile. *Soil and Founds*, **49**(5): 661–673

Liu, T. (2018). *Advanced laboratory testing for offshore pile foundations under monotonic and cyclic loading.* Doctoral dissertation, Imperial College London.

Puech, A., & Garnier, J. (Eds.). (2017). *Design of Piles Under Cyclic Loading: SOLCYP Recommendations*. John Wiley & Sons.

Rimoy, S, Jardine, R, & Standing, J. (2013). Displacement response to axial cycling of piles driven in sand. *Proceedings of the ICE - Geotechnical Engineering*, **166**(2), pp 131–146.

Rimoy, S. (2013). *Ageing and axial cyclic loading studies of displacement piles in sands*. Doctoral dissertation, Imperial College London.

Rimoy, S., Silva, M., Jardine, R., Foray, P., Yang, Z., Zhu, B. & Tsuha, C. (2015). Field and model investigations into the influence of age on axial capacity of displacement piles in silica sands, *Géotechnique,* **65** (7); pp 576 –589.

Salgado, R., Mitchell, J. K., & Jamiolkowski, M. (1998). Calibration chamber size effects on penetration resistance in sand. *Journal of Geotechnical and Geoenvironmental Engineering*, **124**(9), pp 878-888.

Silva, M (2014). *Experimental study of ageing and axial cyclic loading effect on shaft friction along driven piles in sand. Doctoral dissertation*, Université de Grenoble. https://tel.archives-ouvertes.fr/tel-01204765

Yang, Z. X., Jardine, R. J., Zhu, B. T., Foray, P., & Tsuha, C. H. C. (2010). Sand grain crushing and interface shearing during displacement pile installation in sand. *Géotechnique*, **60**(6), pp 469–482.

Zhu, B., Jardine, R., & Foray, P. (2009). The Use of Miniature Soil Stress Measuring Cells in Laboratory Applications Involving Stress Reversals. *Soils and Foundations*, **49**(5), pp 675–688.